SPATIOTEMPORAL MEASUREMENT OF LIGHT EXTINCTION COEFFICIENTS IN COMPARTMENT FIRES

Lukas Arnold[1] l.arnold@fz-juelich.de
Alexander Belt[1] a.belt@fz-juelich.de
Thorsten Schultze[2] schultze@nts.uni-due.de
Lea Sichma[2] lea.sichma@uni-due.de

[1] Institute for Advanced Simulation, Forschungszentrum Jülich, Germany
[2] Communication Systems, University Duisburg-Essen, Germany

INTRODUCTION

In the assessment of life safety in complex building structures in case of fire visibility is one of the main tenability criteria in performance based design. Especially if the orientation of the occupants depends on the perception of signs and doors[1], a sufficient visibility is crucial. Both aspects, i.e. visibility as a tenability criterion and as a limiting factor for the orientation, manifest in the ASET-RSET[2] concept. Here, visibility will reduce the available safe egress time[3,4] and due to reduction of walking speed or prolonged orientation and route evaluation[5] it will increase the required safe egress time. As modern fire safety analysis is based on computer simulations, e.g. using the Fire Dynamics Simulator (FDS[6]), a valid prediction of the smoke spread and especially its light attenuation must be achieved.
The determination of visibility is basically based on a threshold for the intensity of the perceived light. As the light travels from the object, e.g. an illuminated sign, to the observer, its intensity may be reduced due to an interaction with the medium between both. The kind of interaction, e.g. scattering or absorption, as well as its amplitude and dependence on wavelength are subject to the type and number of particles in the medium. While the particle density n has mainly an impact on the amplitude, the predominant is given by the properties of the particles. The latter aspect is effectively described by an interaction, here mainly the extinction cross section c_{ext}. Its value and the value of quantities defined further down depend on the wavelength of the light. However, this will not be further distinguished in this paper and implicitly assumed that they all are wavelength dependent, without additional naming.
As a light ray travels along the line-of-sight, its initial intensity I_0 is in general reduced. The transmission T describes the ratio of the reduced intensity I and I_0. Using the Beer-Lambert law (equation 1), the transmission can be expressed as a function of the optical depth τ.

$$T = \frac{I}{I_0} = \exp(-\tau) \qquad [1]$$

In a homogeneous medium with a particle density n and an extinction cross section c_{ext} the optical depth τ is proportional to the distance along the line-of-sight Δs (equation 2).

$$\tau = c_{\text{ext}} \cdot n \cdot \Delta s = \sigma \cdot \Delta s \qquad [2]$$

A further simplification is the definition of the extinction coefficient σ which represents the product of n and c_{ext}, see above equation 2. This leads to only a single physical quantity to be measured in order to describe the light attenuation, as the other one, the distance Δs, is purely geometrical. A summary of the relevant processes and optical properties of smoke can be found in the SFPE handbook of fire protection engineering[7,8].

A common approach to measure the light extinction is an apparatus which combines a light transmitter and receiver. Eventually, both are close to each other, while a light beam is send out and reflected back with a mirror. This is the basic setup of the MIREX[9] measurement system. It uses infrared light which is send across a distance of 2 m. This apparatus can be used to precisely measure the light extinction at a localised, yet one meter wide, position. The usage of multiple devices would allow a spatially resolved measurement, however it would increase the cost and impact the fluid dynamics due to the physical extension of the apparatus. However, the measured data can be used for localised comparison with the results of the presented approach.
In this paper a simple technique to measure the extinction coefficients σ in the range of visible light is proposed. The implicit measurement leads to spatially, here in vertical direction, and temporally resolved data. One of the fundamental assumptions is a layered structure of the smoke. The final goal is to provide spatiotemporal data as a validation basis for the computation of light extinction processes in compartment fires.
The outline of this paper is as follows. First one of the conducted experiments is presented. Its data will be used as example data for the following methodology section. The presented methodology is split into the raw data capturing, the data post-processing and the determination of the extinction coefficients. Finally, two application examples are shown and conclusions and future work are stated.

EXPERIMENTAL SETUP

This section outlines the main characteristics of the experimental setup. The experimental data is used in the following sections to demonstrate the methodology and to provide an application example. The experiment took place in the Heinz-Luck fire detection laboratory at the university of Duisburg-Essen, Germany. The compartment is of cuboid shape with a variable ceiling height. The wall to wall distances are about 10 m, while the ceiling height was chosen to 3.37 m. As the hall is mainly used for testing purposes following the European standard EN 54[10], the laboratory conditions are well known and the presented setup is similar to it. Figure 1a depicts the location of the objects of interest: a pool fire, a camera, a MIREX apparatus and a vertical LED strip. In the following only the placement of the camera is important, which is at a height of 2.3 m and at a distance of 4.4 m from the LED strip. A photo of one of the experiments is shown in figure 1b.

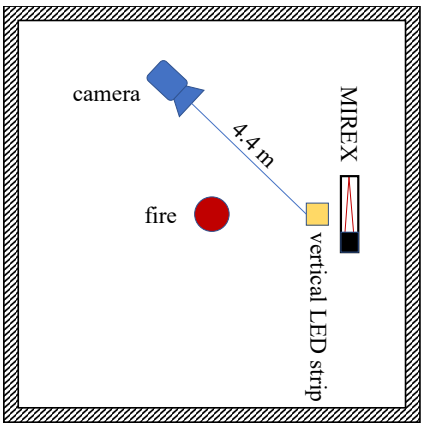

(a) Floor plan of the experimental setup. The main objects are the pool fire, the LED-strip, the MIREX and the camera.

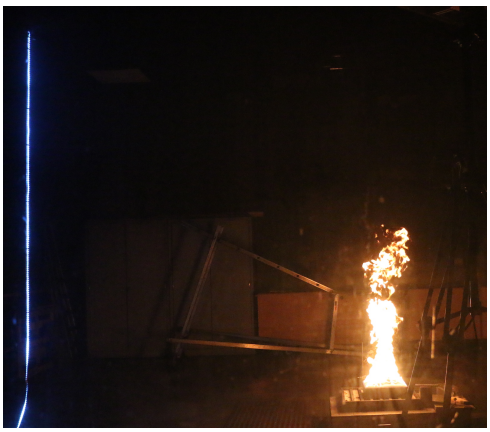

(b) Impression of test fire TF5. The LED strip is visible, while the camera is located on the right hand side.

Figure 1: Experimental setup following the European standard EN 54.

The LED strip used in the experiment is a common consumer product. It is build out of 5 cm long parts which contain three LED units, see figure 2a. The units separation distance is $5/3$ cm, i.e. about 1.67 cm. Each of the units has three individual LEDs which emit red, green and blue light and are therefore capable to produce light in combination of those, see figure 2b. Additionally, it is possible to control the intensity

of a LED. In the presented experiments the LED units are set to white, i.e. all LEDs are on, with the maximal intensity. The length of the vertically aligned strip was 2.35 m, starting about 5 cm below the ceiling and it contained 141 LED units.

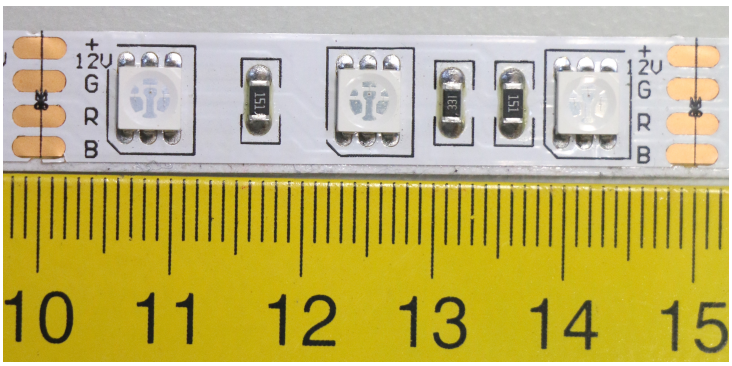

(a) LED turned off. Length units are in cm.

(b) LED turned on.

Figure 2: Physical extension of a LED unit and location of the LED dots.

The fire was one of the fires defined in EN 54 as TF5. It is a pool fire with n-heptane as fuel. In contrast to the norm the amount of fuel was reduced to 500 g which lead to a burning duration of about 3 min. The choice of this fire type is due to the fact that it is the most simple one to be modelled with numerical simulation methods, as it does not involve pyrolysis and the combustion reaction is consuming a single pure fuel.
Figure 3 shows the time line of the experimental procedure. The timing in this run was as follows:

- $t = 0$ s start of the experiment
- $t \sim 30$ s ignition of the pool fire
- $t \sim 200$ s all fuel is consumed, the fire is off
- $t \sim 420$ s hall's ventilation system is turned on
- $t \sim 1200$ s end of the measurements, end of the experiment

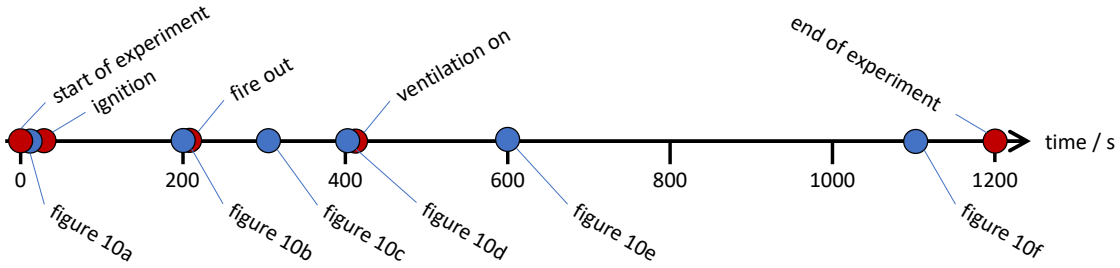

Figure 3: Time line of the experimental procedure. The red dots indicate important time points of the experiment while the blue ones show the time points of figure 10.

The examples in the following methodology section are based on experimental data gathered in the above stated experimental run.

METHODOLOGY

The presented methodology is split into three aspects. The first subsection outlines a few recommendations of the raw data acquisition, while the second one describes the procedure to model the image of each LED unit and thus find its position and determine its intensity in an image frame. In the last subsection a method to discretise the compartment volume into homogeneous smoke layers and the determination of the light attenuation coefficients is introduced.

Raw data acquisition

The methodology is based on the analysis of photo images captured by a camera. During the experiment, the camera continuously captures the LED strip. As the scientific quality of the images is crucial, the settings of the camera are stated and discussed here.
The used camera was a Canon 80D with a Canon 18 mm to 35 mm lens. It was run in full manual mode, i.e. without any brightness corrections or other adjustments. The choice of a manual mode is important as otherwise the camera would adjust its parameters in order to take well balanced images. This would introduce luminosity changes of the LEDs which are not due to light attenuation but due to changes in the camera settings. The images are stored in the common jpeg format as well as in a raw format. The latter one can be used to further increase the accuracy of the analysis as it offers a higher luminosity resolution.
In the manual mode of the camera, all relevant parameters must be manually set. The objective is to have all LED units in focus and the image of the initial signal should be as bright as possible without saturating the CCD chip. In this specific setup the focal ratio was set to 16 in order to achieve a long depth of field, i.e. have all LED units in focus. With a low ISO number of 100 – to reduce the CCD noise – the resulting exposure time was $1/500$ s. With a distance to the LED strip of about 4.4 m and a focal length of 18 mm, each pixel of the image corresponds to a distance of about 0.88 mm on the LED strip. Using a programmable remote control, the camera took a picture every second.
Figure 4 shows a part of a baseline image, i.e. taken just before the experiment started. Each colour image is a combination of three channels, representing the red, green and blue colour contributions. The very left subfigure shows the common RGB (red/green/blue) representation of the image and the other figures depict the individual channels. The value range, here of the jpeg file format, uses 256 integer values for each channel. The red and green channels do not reach the saturation value of 255, however, the blue one is reaching this value and is therefore saturated. Here, the blue channel can not be used for a scientific evaluation as the actual brightness level is not captured by the CCD.

Determination of LED dot positions

Once the images are taken, the position and intensity of all LED units needs to be found. This is done in two phases: First, and only once per experiment, search areas are fixed. Second, an image model is fitted to each individual image of all LED units. The result is a list with various properties, like intensity or position, for all units on the strip. In the following the analysis is demonstrated only for one, here red, channel.
In the first phase, search areas for each LED unit are identified. This is done only once and is based on a reference image, e.g. taken just before the experiment started. It is assumed that all available LED units are clearly visible on the image. Here a simple maximum search is conducted. For the found maximum a pixel range, the search area, is defined. This area is excluded during the search for the next maximum. This procedure is repeated until all maxima, which are well above the mean value, are found. The width of the search area depends on the pixel separation of the LED units on the image. In the presented case, the width was set to 20 pixel. To ease the automated analysis, it is possible to exclude defect or partly covered LED units from further analysis. It should be noted, that the definition of the search areas must happen on the reference frame as during the experiment the LED unit image may become very dark or even vanish. In this case the analysis would miss the important information of an highly attenuated signal.

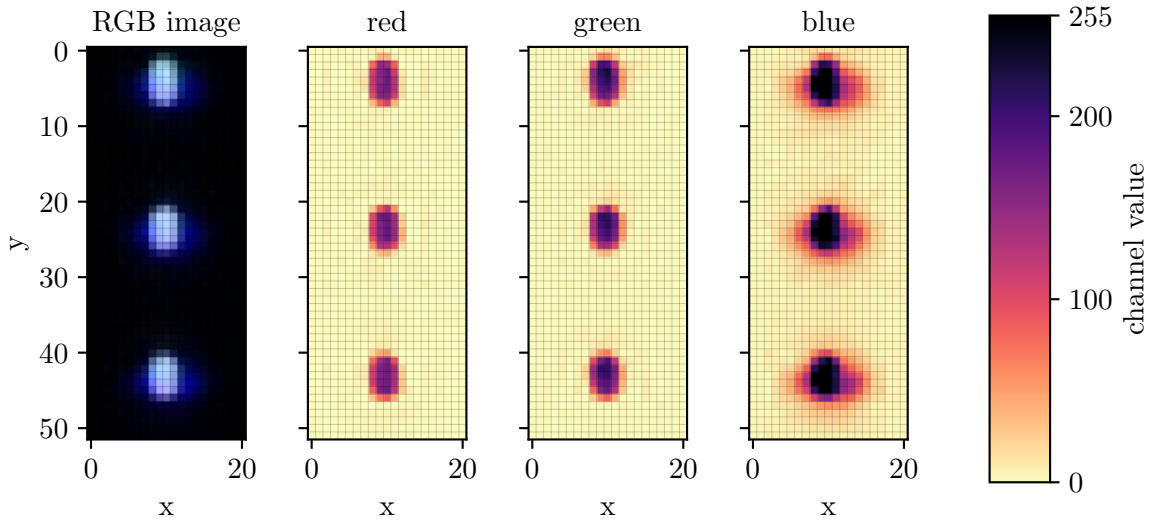

Figure 4: Zoomed area of three LED units on a reference image frame. The image on the very left shows the combined RGB colour image, while the following ones show the individual colour channels.

In the second phase a simple image model for a single LED unit is fitted to the individual search areas. The model is based on the assumption that the image can be represented by an algebraic function. The basic structure of the function is as follows. There is a region around the central point at x_0 and y_0 with a nearly constant brightness amplitude A_0. The central region has a radius r_0 and transits smoothly towards zero within the width w. However, the LED unit images are asymmetric. Therefore, the radius r_0 and the width w can be defined as two components in the x- and y-direction, i.e. $r_{0,x}$, $r_{0,y}$, w_x and w_y. Additionally, a rotational angle α can be defined. In total this are eight parameters: A_0, x_0, y_0, $r_{0,x}$, $r_{0,y}$, w_x, w_y and α. The explicit formula for the value A_m of a pixel at position x, y in the model image is given in equation 3.

$$A_m(x,y) = A_0 \cdot \frac{1}{2}\left(1 - \tanh\left(\frac{r(x,y) - r_0(x,y)}{w(x,y)}\right)\right) \quad [3]$$

With the radius r defined as

$$r(x,y) = \sqrt{(x-x_0)^2 + (y-y_0)^2} \quad [4]$$

and the polar angle ϕ

$$\phi(x,y) = \arctan\left(\frac{y}{x}\right) + \alpha \quad \text{with the according quadrant adoptions} \quad [5]$$

the central region $r_0(x,y)$ and the width $w(x,y)$ can be computed as a function of the above defined polar coordinates

$$r_0(x,y) = \frac{r_{0,x} r_{0,y}}{\sqrt{(\sin(\phi) r_{0,x})^2 + (\cos(\phi) r_{0,y})^2}} \quad [6]$$

$$w(x,y) = \frac{w_x w_y}{\sqrt{(\sin(\phi) w_x)^2 + (\cos(\phi) w_y)^2}} \quad . \quad [7]$$

Figure 5 provides three examples of equation 3. It demonstrates a symmetric image with a extended central region (left), an inclined asymmetric image (middle) and a blured image (right).

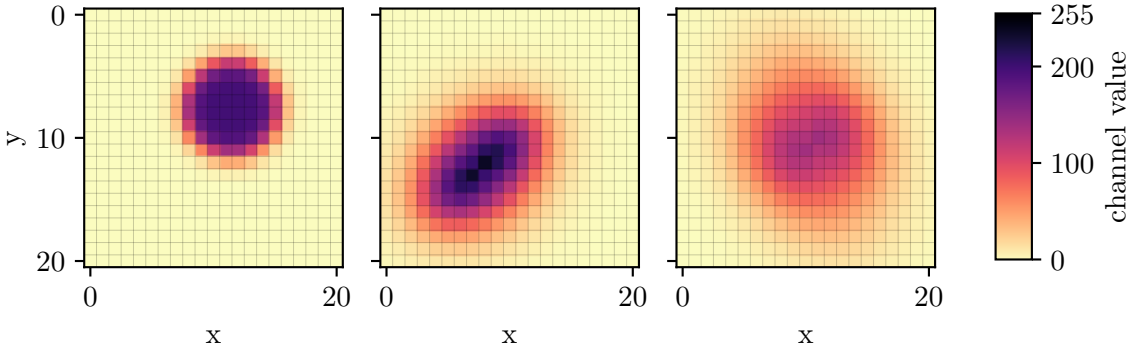

Figure 5: Examples of equation 3.

To find the best fitting parameters a minimisation algorithm is used. The cost function Ω_{LED} is the L2-norm of the pixel values (one channel) of the experimental image A_e within the search area and the modelled intensity $A_m(x,y)$ on the same pixel area:

$$\Omega_{\text{LED}} = \sqrt{\sum_{\text{all pixels } i,j} (A_e(i,j) - A_m(i,j))} \quad . \tag{8}$$

Additionally, penalty terms are defined to ensure that the central points are within the search area and the amplitude, radii and widths are positive.
Figure 6 shows an example, where an individual LED unit image (left) is fitted by the model image (middle). The best fitting parameter values for this LED unit image are: $x_0 = 11.01$, $y_0 = 12.32$, $r_{0,x} = 1.75$, $r_{0,y} = 2.91$, $A_0 = 170.11$, $w_x = 0.77$, $w_y = 0.72$, $\alpha = 0$. The overlay of both images (right) illustrates the reasonable matching of the original image. It should be noted that this approach is capable of detecting small movements and changes in the intensity, as the model is not bound to the discrete channel and position, i.e. pixel, values.

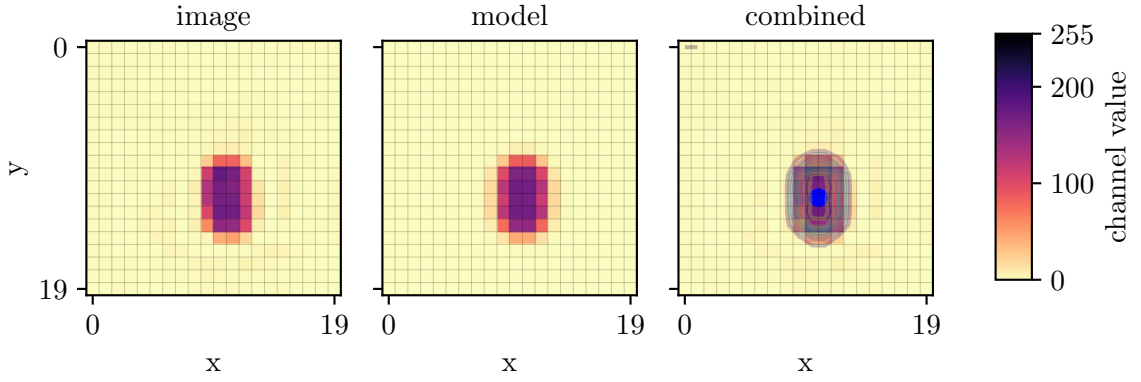

Figure 6: Fitting example for a single LED unit.

Finally, this process is repeated for all LED units and all frames taken. The results are time lines for each model parameter of each LED unit. To demonstrate the resulting data, a few selected time lines for three LED units, located at a low, middle and upper position on the LED strip, are shown in figure 7. Subfigure 7a shows the change in the amplitude A_0 during the experiment. The LED unit at the upper position shows the largest drop in intensity. The y-coordinate of the central point y_0, subfigure 7b, shifts synchronously for all LED units on a scale of two pixels in the captured frames, yet a clear dynamics is detectable. While the parameters $r_{0,y}$ and w_y of LED unit in the lower position show only little change, the other ones show an evolution along the course of the experiment. In both cases the central region

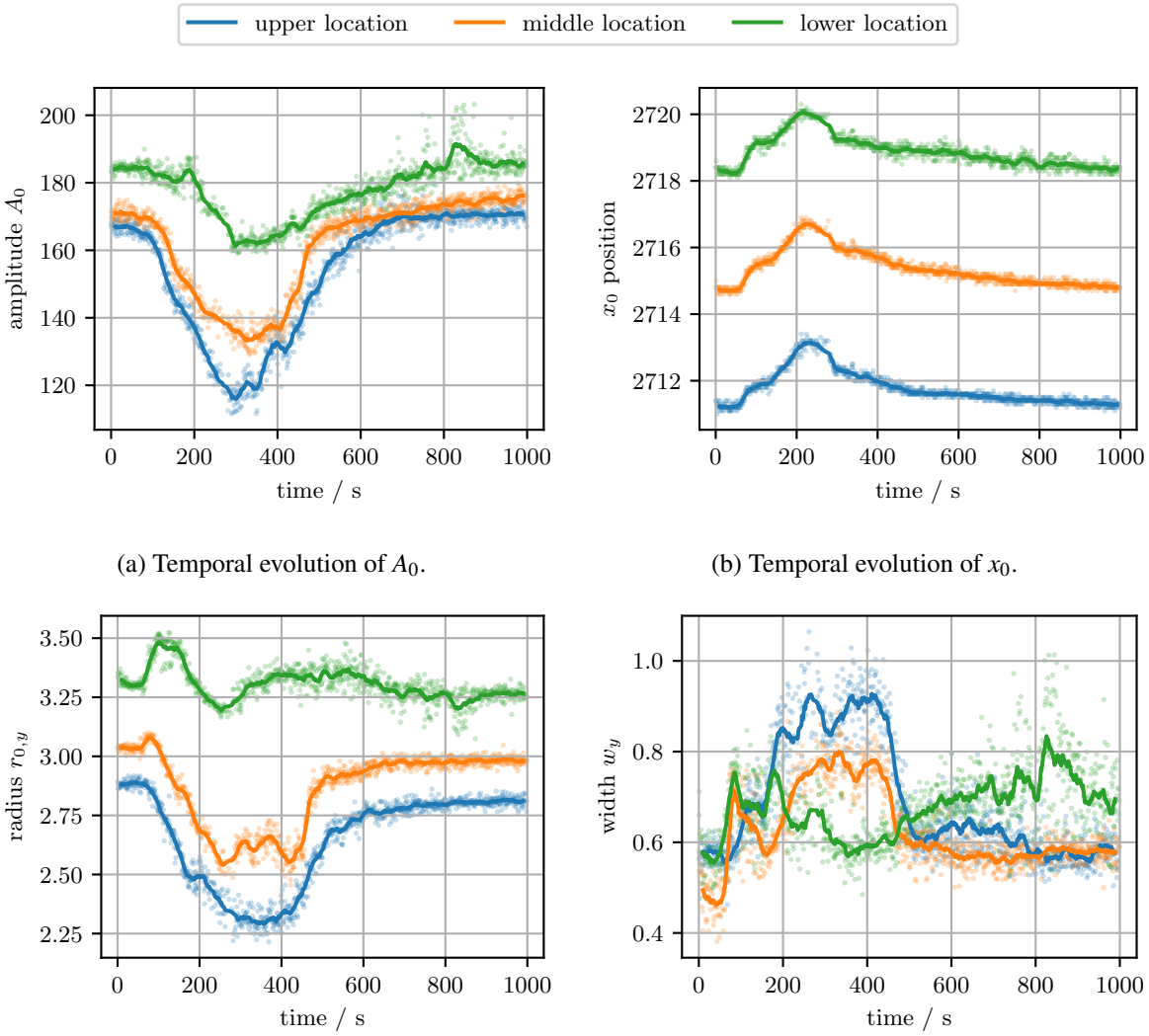

(a) Temporal evolution of A_0.

(b) Temporal evolution of x_0.

(c) Temporal evolution of $r_{0,y}$.

(d) Temporal evolution of w_y.

Figure 7: Temporal evolution of model parameters for three selected LED units.

becomes smaller while the transition region grows, i.e. the shape becomes refocused. Towards the end of the time series the values of all parameters and LED units tend towards the initial values.

Computation of extinction coefficients

The final goal of the presented method is to gain spatially resolved information of the extinction coefficients. As described in the following, a simple model based on spatial discretisation, here in horizontal layers, is outlined. Using the captured intensities, based on the amplitude parameter A_0 in equation 3, a best matching set of extinction coefficients is determined. This approach applies the line-of-sight integral of the Beer-Lambert law in an inhomogeneous medium.
The proposed model is has the following assumptions:

1. the light absorption properties, i.e. σ, in a layer is homogeneous,
2. the plume region is neglected,
3. light paths are linear, e.g. refraction due to varying gas temperatures is neglected, and
4. only the product $\sigma = c_{\text{ext}} \cdot n$ in equation 2 is determined.

The severity of these assumptions is different for each one. While the assumption of homogeneous layers may be critical for complex compartments, neglecting of the plume region will be a minor issue for sufficiently large spaces. Refraction will have a minor role for low energy fires, like smouldering, as the involved temperatures are just above the ambient. Finally, the capability to distinguish between c_{ext} and n is not critical for the computation of visibility, as the the optical depth depends only of their product σ.
The model's data structure is a set of N_{layers} extinction coefficients σ_i. They represent the values at homogeneous horizontal layers which fill the domain of interest, e.g. a compartment, see figure 8. As the light rays travel from one of the N_{LEDs} LED units L_j to the camera it passes one or more of the layers. The height of the layers Δh_i does not have to be equal, however it is kept constant in this contribution.

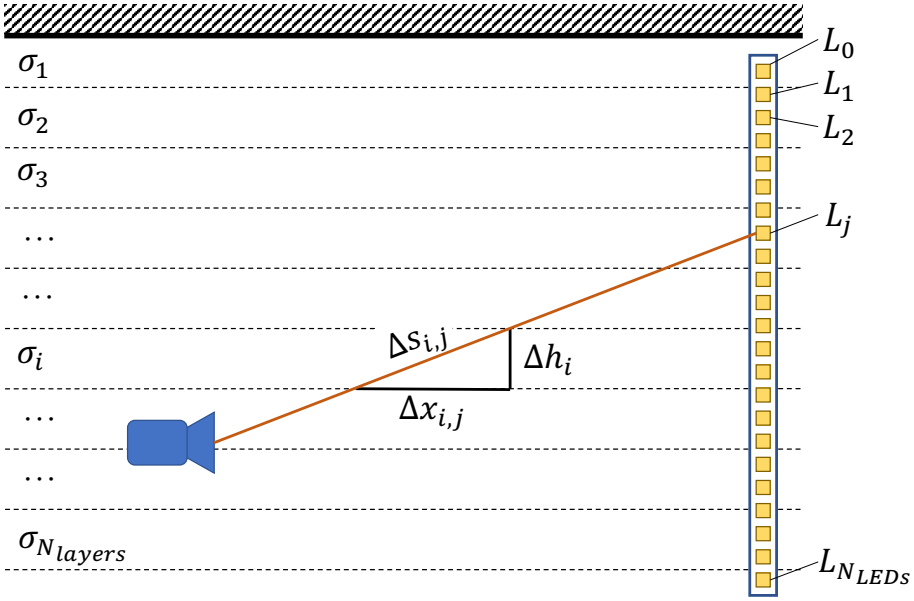

Figure 8: Schematics of the layer model. Each layer corresponds to a constant extinction coefficient σ_i. The LED units L_j are not aligned to these layers. The light rays from a LED unit to the camera pass individual layers, where $\Delta s_{i,j}$ indicates the path length travelled by the light emitted by the unit L_j in the i-th layer.

In order to evaluate the Beer-Lambert law, the path of each straight light ray across the layers have to be determined. The path between the camera and the LED unit L_j is computed using fundamental geometry. This results in path lengths $\Delta s_{i,j}$ for the light ray travelling from the j-th LED unit thought the i-th layer. If the light ray does not cross a layer, the corresponding value is set to zero.
The determination of the extinction coefficients σ_i is based on the general form of the Beer-Lambert law for an inhomogeneous medium. Equation 9 demonstrates the integration along the path s.

$$\tau = \int_s c_{\text{ext}} n(s)\, \mathrm{d}s = \int_s \sigma(s)\, \mathrm{d}s \qquad [9]$$

The usage of discrete layers with constant constant values simplifies this integral into a finite sum over all layers, using the computed travel paths $\Delta s_{i,j}$ and the yet to be determined extinction coefficients σ_i, see equation 10.

$$\tau_j = \sum_{i=1}^{N_{\text{layers}}} \sigma_i \Delta s_{i,j} \qquad [10]$$

In the following all intensities are scaled to their initial values I_0 and thus range from zero to one. The

experimental intensities I_e are scaled by the mean of ten reference images taken just before the experiment started. The modelled intensities $I_{m,j}$ of L_j are given by equation 11.

$$I_{m,j} = \exp\left(-\sum_{i=1}^{N_{\text{layers}}} \sigma_i \Delta s_{i,j}\right) \quad [11]$$

Equation 12 poses an equation system, containing N_{LEDs} non-linear equations, to be solved for σ_i. This system has to be solved for each frame, however, the travel paths $\Delta s_{i,j}$ are computed only once, as they do not change in time.

$$I_{m,j}(\sigma_0, \ldots, \sigma_{N_{\text{layers}}}) = I_{e,j} \quad \text{for all} \quad j \in [1, N_{\text{LEDs}}] \quad [12]$$

In order to solve the target equation system, a minimisation procedure is used. This has the advantage, that additional criteria, but solely the distance between the experimental and modelled data, can be defined. Therefore, a cost function Ω_σ is defined as shown in equation 13.

$$\Omega_\sigma = \sum_{j=1}^{N_{\text{LEDs}}} (I_{m,j} - I_{e,j})^2 + \phi_s \sum_{i=2}^{N_{\text{layers}}-1} (\sigma_{i-1} - 2\sigma_i + \sigma_{i+1}) + \phi_a \sum_{i=1}^{N_{\text{layers}}} \sigma_i \quad [13]$$

It is a sum of three contributions. The first one computes the L2-norm between the experimental and modelled data for all LED units. The second one represents the requirement of a smoothness of the solution, here the numerical approximation of the second derivative. In order to prevent individual high peaks, the weighting factor ϕ_s can be set to a non-trivial positive value to favour low curvatures. The last term controls if the minimisation process prefers high or low values of the extinction coefficients, depending of the sign of the weighting factor ϕ_a. This option is essential to capture a range of possible values for σ_i in cases where there is little impact on the L2-Norm. For example, if the LED signal was damped to nearly zero, there is a minimal value for the extinction coefficient to achieve this results. However, the actual value may be significantly higher. In order to quantify these effects, the sign of ϕ_a can be accordingly chosen.

An example of the outcome of the above optimisation procedure is given in figure 9. This figure contains a set of results, which are distinguished by the number of extinction coefficient layers N_{layers} in equation 10. For each of the results, the vertical distribution of extinction coefficients is shown (left hand side) as well as the corresponding modelled intensity I_m (right hand side). First, the model is capable to represent the experimental intensities (grey dots) within the variation of the data. All N_{layers} lead to very similar curves. Second, also the extinction coefficients follow a similar shape. The curves with higher numbers of layers show more features, which are not necessary physical but may be artefacts of a more accurate fitting of the noisy data. Third, the extinction coefficients above about 3.35 m drop towards zero. This is due to the fact, that the cost function, equation 13, favours small extinction coefficients. As there is no experimental data for this heights – the top LED unit is at about 3.35 m – this leads to small or even zero coefficients. Each layer of the low N_{layers} numbers covers a larger portion of the space and therefore does not include layers which are not crossed by any light paths.

APPLICATION EXAMPLE

As the focus of this contribution is the methodology, this section presents just two selected aspects of the data analysis. These are the temporal evolution of the extinction coefficient layers and the comparison to a MIREX measurement.

First, the development of the light attenuation in the layers is depicted in figure 10 for six selected points in time. The selected times are outlined in figure 3 and are chosen to capture the main dynamic of the experiment. At the beginning of the experiment, i.e. $t = 0$ s, all extinction coefficients are nearly zero. The following three snapshots show a build up of a layer with increasing extinction coefficients. Especially at $t \sim 300$ s a layering with a smooth shape from zero at the lower layers towards the maximum at the highest point can be observed. Once the ventilation system is activated the layering is significantly

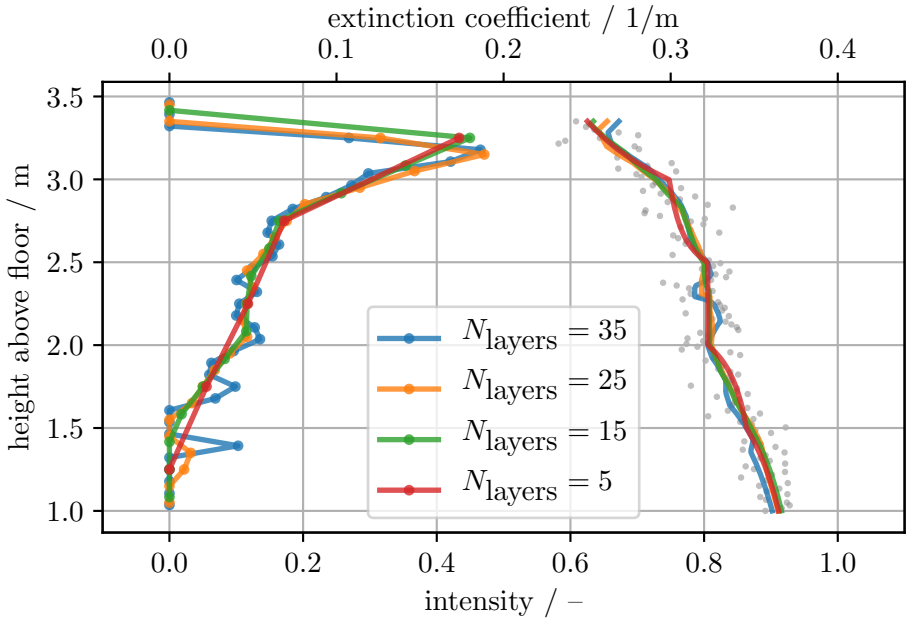

Figure 9: Comparison of models with varying number of layers N_{layers}. The lines on the left correspond to the extinction coefficients, while those on the right show the model output for the LED unit intensity I_m. Experimental intensities I_e are represented by grey dots.

reduced ($t \sim 600\,\text{s}$) and eventually drops to the initial (zero) state, as shown for $t \sim 1100\,\text{s}$. Although this experiment does not provide new insights, this result demonstrates the capturing of the spatiotemporal evolution of the extinction coefficient.

Second, the results of the data analysis are compared to MIREX measurements. It is important to note, that the data is not directly comparable as the MIREX measures the light extinction in the infrared regime while the results shown here are for red light. But nevertheless both measurements are compared to identify trends and orders of magnitude. Figure 11 shows the temporal evolution of the extinction coefficient measured by the MIREX and of the new approach at the position – here the height – of the MIREX. In this figure two data sets of the measurements based on the LED technique are shown. One is the result of an optimisation where low extinction coefficients are favoured, positive ϕ_a in equation 13. A second one where high values are favoured, negative ϕ_a. This is necessary as the MIREX is located just above the ceiling, i.e. in the top layers of the model which have the highest uncertainty as only few light paths cross them. With this approach, a kind of upper and lower limit for the extinction coefficients is estimated, where both limits still lead to reasonable representation of the experimental data. The comparison of both measurements demonstrates that the proposed method is able to capture the dynamics as well as the amplitude of the extinction coefficient the same way as the MIREX measurement. However, the MIREX system seems to be more sensitive, i.e. indicates higher extinction coefficients, in the initial phase and in the decaying phase.

CONCLUSIONS

This paper presents an approach to capture the light attenuation of individual LED units in a compartment fire. Using this approach multiple quantities, like mainly the amplitude but also the position and broadening of the signal, can be captured on a scale which is finer than the colour level or the pixel width. This accuracy allows to include further effects, like refraction, into the analysis. The determination of the extinction coefficients is based on a simple method and is therefore expected to be robust with respect to the failure of individual LEDs or small movements of the strip. However, the validation needs further investigation to find a more conclusive comparison method with other techniques. Although, the

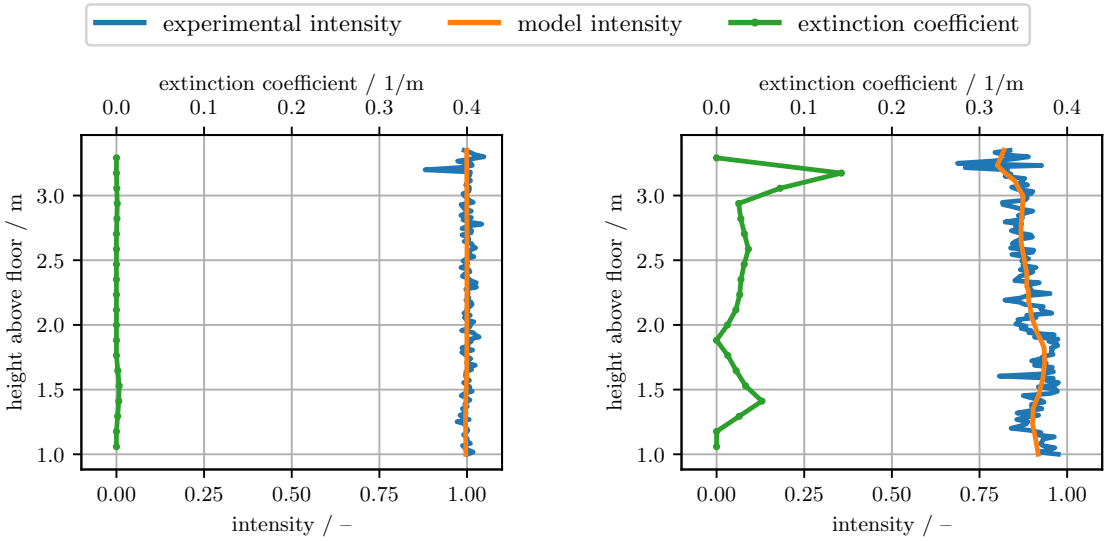

(a) $t = 0\,\mathrm{s}$.

(b) $t \sim 200\,\mathrm{s}$.

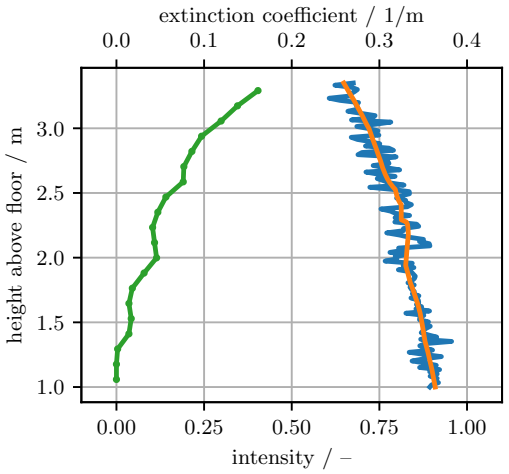

(c) $t \sim 300\,\mathrm{s}$.

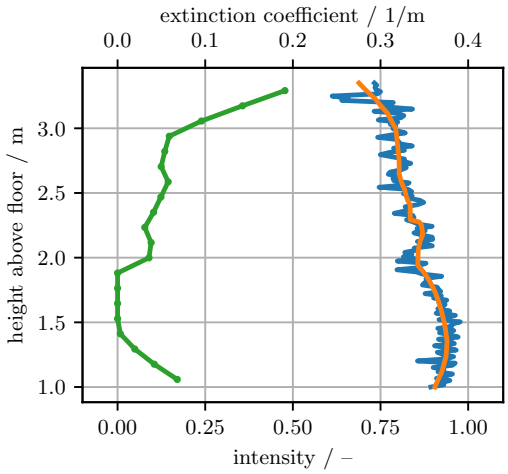

(d) $t \sim 400\,\mathrm{s}$.

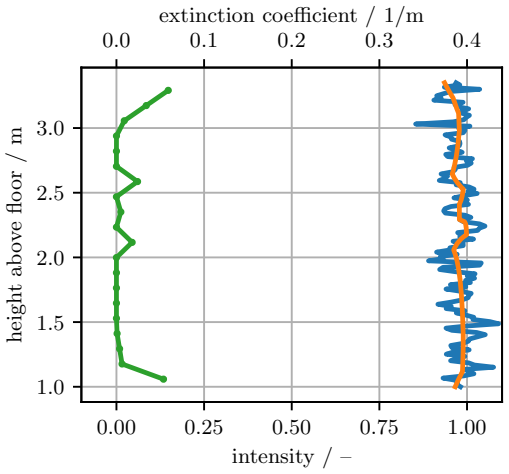

(e) $t \sim 600\,\mathrm{s}$.

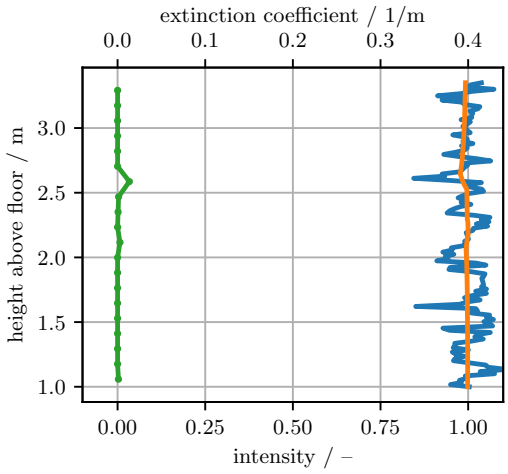

(f) $t \sim 1100\,\mathrm{s}$.

Figure 10: Temporal evolution of the extinction coefficient layers at six selected points in time, see figure 3.

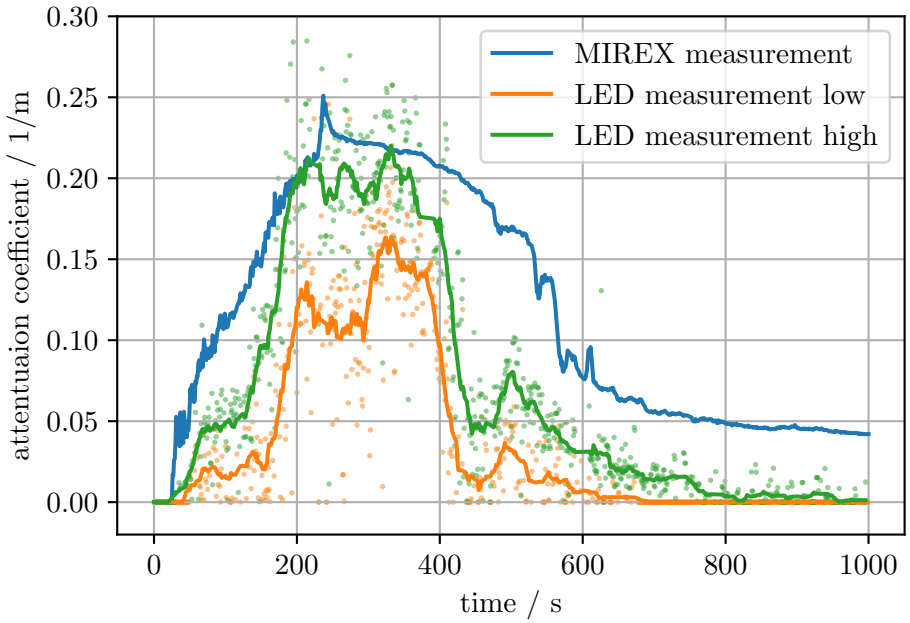

Figure 11: Comparison of a MIREX measurement with the results of the presented approach. The data based on the LED measurement shows the results of an optimisation towards low as well as high extinction coefficients.

comparison with the MIREX data is promising, more suitable measurement locations must be revised as well as the impact of the wavelength, here between infrared and red, must be evaluated. Eventually, the analysis with the LED light, which targets wavelengths in the visible spectrum, may lead to more applicable extinction coefficients.
The instantaneous capturing of spatially resolved extinction coefficients, especially in the visible spectrum, will provide a validation basis for numerical tools. Especially as it generates data for inhomogeneous distributions, so that transport processes can be evaluated as well. The general approach will allow an application on small scale as well as on large scale, as long as the assumptions are expected to be valid. This shows the need of providing a method to check the validity with experimental methods.
In terms of applicability, the proposed method is easily applicable at low cost. This is due to the usage of consumer products and no need for fine tuning or calibration with external sources. The most part of the process is covered by the data analysis. As the analysis is written in Python and can be freely shared with others – please contact the authors to gain access – it can be directly applied by others researchers.

OUTLOOK

As pointed out in the conclusions, there exists a range of topics to improve the validity and applicability of the proposed method and a few of them are subject of current research.
One of the main tasks is to investigate other fire types, but solely TF5. In this contribution it was chosen as one of the simplest. However, especially in case of weak thermal drivers, like in case of smouldering, the dynamics will be more challenging to be captured and the gained spatial resolution will be of high importance for model validation.
To address the question of homogeneous layers, multiple LED strips and two (or more) cameras can be used. This will allow investigating the variations along the smoke layers. In combination with additional MIREX measurements at multiple heights, a broader understanding of the smoke spread, e.g. light extinction coefficients, will be achieved.
Further measurements of other quantities, like gas temperatures, will help to investigate other effects, like refraction. More information on the particles, using measurements of particle density and size

distribution at few locations in the compartment during the fire, will allow to estimate the extinction cross sections. In this way different particle types, due to different combustion, pyrolysis or transport processes, will be distinguished for the various fire types. Thus, this information can be used to estimate the particle numbers, with the assumption of a known c_{ext}, as well as the difference of infrared and red light measurements.
Finally, numerical simulations with FDS will be carried out. The results of theses simulations will be used to investigate the homogeneity assumptions in combination with a comparison the measured (LED and MIREX) extinction coefficients. In case of fire type TF5, all relevant quantities, like the mass loss rate, have been captured. Thus a design fire will be sufficient to represent the evaporation process.

REFERENCES

[1] Erik Andresen. *Wayfinding and Perception Abilities for Pedestrian Simulations*. PhD thesis, Bergische Universität Wuppertal, 2018.

[2] Leonard Y. Cooper. A concept for estimating available safe egress time in fires. *Fire Safety Journal*, 5(2):135 – 144, 1983.

[3] Wojciech Węgrzyński and Gabriele Vigne. Experimental and numerical evaluation of the influence of the soot yield on the visibility in smoke in cfd analysis. *Fire Safety Journal*, 91:389 – 398, 2017.

[4] Benjamin Schröder. *Multivariate Methods for Life Safety Analysis in Case of Fire*. PhD thesis, Bergische Universität Wuppertal, 2016.

[5] Benjamin Schröder, David Haensel, Mohcine Chraibi, Lukas Arnold, Armin Seyfried, and Erik Andresen. Knowledge- and Perception-based Route Choice Modelling in Case of Fire. In *6th International Symposium on Human Behaviour in Fire 2015*, 2015.

[6] Kevin McGrattan, Simo Hostikka, Randall McDermott, Jason Floyd, Craig Weinschenk, and Kristopher Overholt. *Fire Dynamics Simulator User's Guide, version 6.7.1*, 2019.

[7] G. W. Mulholland. *SFPE Handbook of Fire Protection Engineering*, chapter Smoke Production and Properties. 3 edition, 2002.

[8] Jeffrey S. Newman, Geary G. Yee, and Paul Su. *SFPE Handbook of Fire Protection Engineering*, chapter Smoke Characterization and Damage Potentials. 5 edition, 2016.

[9] CERBERUS LTD. *Extinction measuring equipment MIREX, Technical description*, 1991.

[10] The European Committee for Standardization. *EN 54, Fire detection and fire alarm system*.